References and Notes

1. C. S. Hill and R. Treisman, *Cell* **80**, 199 (1995); M. Mannervik *et al.*, *Science* **284**, 606 (1999); K. Struhl, *Cell* **98**, 1 (1999).
2. T. E. Crowley *et al.*, *Nature* **361**, 557 (1993).
3. S. K. Hansen *et al.*, *Cell* **91**, 71 (1997).
4. V. Orlando and R. Paro, *Cell* **75**, 1187 (1993). Cells were treated for 15 min at 25°C with 1% formaldehyde (final concentration). After lysis with a buffer containing 50 mM Hepes (pH 7.6), 140 mM NaCl, 1 mM EDTA, 1% Triton X-100, 0.1% Na-deoxycholate, and 0.5 mM phenylmethylsulfonyl fluoride (PMSF), the resuspended nuclear pellets were sonicated four times for 30 s to shear the chromatin into fragments averaging 500 bp. The fragmented chromatin extract was dialyzed into a 3 M urea solution to dissociate TRF1-associated factors and non-crosslinked DNA-bound proteins. The extracts were spun for 15 min at 15,000*g*, the urea was dialyzed out, and the extracts were respun. Each precipitation was performed with extracts from 1.5×10^8 cells. The extracts were precleared for 1 hour with protein A–Sepharose beads (Amersham Pharmacia). The beads were removed, and the immunoprecipitations were carried out overnight with 2 μg of antibody and 15 μl of protein A–Sepharose beads. The beads were washed six times with lysis buffer and six times with a buffer containing 0.1 M tris-HCl (pH 7.9), 0.5 M LiCl, 1% NP-40, 1% Na-deoxycholate, and 0.5 mM PMSF. The antibody-antigen complexes were eluted and the crosslinks were reversed. The proteins were treated with proteinase K and the DNA isolated by phenol-chloroform extraction and ethanol precipitation. The DNA was radiolabeled by random priming using the Klenow fragment and random hexameric primers in the presence of cold deoxynucleotide triphosphates and [α-^{32}P]deoxycytidine triphosphate and then used to probe DNA hybridization blots containing restriction fragments of the *tudor* and AntP1 promoters.
5. B. P. England, U. Heberlein, R. Tjian, *J. Biol. Chem.* **265**, 5086 (1990).
6. T. A. Bunch, Y. Grinblat, L. S. Goldstein, *Nucleic Acids Res.* **16**, 1043 (1988).
7. M. C. Holmes and R. Tjian, unpublished data.
8. Y. Sadovsky *et al.*, *Mol. Cell. Biol.* **15**, 1554 (1995); J. Colgan and J. L. Manley, *Genes Dev.* **6**, 304 (1992).
9. S. Takada and R. Tjian, unpublished data.
10. M. C. Holmes, P. Hurban, K. P. White, R. Tjian, unpublished data.
11. M. D. Rabenstein *et al.*, *Proc. Natl. Acad. Sci. U.S.A.* **96**, 4791 (1999); E. Maldonado, *J. Biol. Chem.* **274**, 12963 (1999); T. Ohbayashi, Y. Makino, T. Tamura, *Nucleic Acids Res.* **27**, 750 (1999); E. Wieczorek *et al.*, *Nature* **393**, 187 (1998).
12. R. Dikstein, S. Zhou, R. Tjian, *Cell* **87**, 137 (1996); M. Hiller, T.-Y. Lin, M. Fuller, unpublished data.
13. P. Margolis, A. Driks, R. Losick, *Curr. Opin. Genet. Dev.* **1**, 330 (1991).
14. A. J. Courey and R. Tjian, *Cell* **55**, 887 (1988). The *tudor* and HSV TK promoters were fused to the luciferase reporter gene in the pGL3-Basic vector (Promega). Cells were transiently transfected by the calcium phosphate coprecipitation method. The luciferase reporter constructs were cotransfected with increasing amounts of a pPAC vector expressing either TRF1 or TBP under the actin 5C promoter. The ø lanes are control transfections with only the luciferase reporter constructs transfected. These values were set to 1 to represent the basal level for each promoter. Cells (3×10^6) were transfected with 300 ng of the luciferase reporter construct, 50 ng of a CMV-renilla construct as an internal standard, and 100 ng, 500 ng, or 1 μg of the pPAC vector expressing either TRF1 or TBP. An empty pPAC vector was added to each transfection experiment to bring the total amount of pPAC in each experiment up to 1 μg, and salmon sperm was added to bring the total amount of DNA in each transfection to 5 μg.
15. Recombinant TBP, TFIIA, and TFIIB were purified as described [S. K. Hansen and R. Tjian, *Cell* **82**, 565 (1995); B. F. Pugh and R. Tjian, *Genes Dev.* **5**, 1935 (1991)]. TRF1 was expressed recombinantly in *Escherichia coli* and purified as described (*5*). TFIID, TFIIE, TFIIF, TFIIH, and RNA Pol II were purified from nuclear extracts derived from 0- to 12-hour *Drosophila* embryos. Nuclear extracts were prepared as described [U. Heberlein and R. Tjian, *Nature* **331**, 410 (1988)], dialyzed into 0.1 M KCl HEMG buffer [25 mM Hepes (pH 7.6), 12.5 mM $MgCl_2$, 0.1 mM EDTA, 10% glycerol, 1 mM dithiothreitol, 1 mM PMSF, and 1 mM sodium metabisulfite], and loaded onto a 40-ml Poros 20 HE1 column. The basal factors were stepped off with 0.4 M NaCl HEMG buffer and loaded onto a 520-ml Sephacryl-300 column (S300, Pharmacia) equilibrated in 0.1 M NaCl HEMG buffer. The proteins were resolved isocratically and the fractions assayed for transcriptional activity. TFIID activity was isolated from fractions corresponding to the void volume of the S300 column. Several fractions eluting after the void volume and TFIID were tested and found to contain the TFIIE, TFIIF, TFIIH, and RNA Pol II activities used in the experiments for this study. TFIID was further purified by directly loading the S300 fractions containing TFIID activity onto an 8-ml Mono-Q HR 10/10 column (Pharmacia). TFIID was eluted from the column with a 25-column volume gradient from 0.1 to 0.5 M NaCl in HEMG buffer. TFIID activity eluted between 0.25 and 0.3 M NaCl.
16. K. Yokomori *et al.*, *Genes Dev.* **8**, 2313 (1994).
17. A. M. Maxam and W. Gilbert, *Proc. Natl. Acad. Sci. U.S.A.* **74**, 560 (1977).

18. We thank R. Freiman, C. Inouye, A. Ladurner, A. Hochheimer, J. Ziegelbauer, and D. Rio for critical reading and comments on the manuscript; J. Zwicker for collaborating in setting up a reconstituted in vitro transcription system; S. Takada for stably transformed SL2 cell lines and affinity-purified antibodies to TRF1; R. Jacobson and S. Ryu for reagents; and T. O'Brien for helpful scientific discussions and advice. Supported in part by NIH grant CA25417 (R.T.).

15 November 1999; accepted 6 March 2000

Requirement of JNK for Stress-Induced Activation of the Cytochrome c–Mediated Death Pathway

Cathy Tournier,[1] Patricia Hess,[1] Derek D. Yang,[2]* Jie Xu,[2] Tod K. Turner,[3] Anjaruwee Nimnual,[4] Dafna Bar-Sagi,[4] Stephen N. Jones,[3] Richard A. Flavell,[2] Roger J. Davis[1]†

The c-Jun NH_2-terminal kinase (JNK) is activated when cells are exposed to ultraviolet (UV) radiation. However, the functional consequence of JNK activation in UV-irradiated cells has not been established. It is shown here that JNK is required for UV-induced apoptosis in primary murine embryonic fibroblasts. Fibroblasts with simultaneous targeted disruptions of all the functional *Jnk* genes were protected against UV-stimulated apoptosis. The absence of JNK caused a defect in the mitochondrial death signaling pathway, including the failure to release cytochrome c. These data indicate that mitochondria are influenced by proapoptotic signal transduction through the JNK pathway.

The development and maintenance of healthy tissues involves apoptosis, a program of physiologically regulated cell death (*1*). Dysregulated apoptosis contributes to many pathologies, including tumor promotion, autoimmune and immunodeficiency diseases, and neurodegenerative disorders (*2*). Therefore, signaling pathways that trigger apoptosis are of intense interest. The c-Jun NH_2-terminal kinase (JNK) signaling pathway is essential for neuronal apoptosis in response to excitotoxic stress (*3*). However, the role of JNK in the apoptotic responses of other cell types is unclear. The goal of this study was to define the requirement for JNK in apoptosis of primary murine embryonic fibroblasts (MEF).

MEF were prepared from wild-type (WT) embryos and mutant embryos in which the *Jnk* genes were disrupted (*3, 4*). WT MEF expressed large amounts of 46-kD JNK1 and 55-kD JNK2 isoforms and small amounts of 55-kD JNK1 and 46-kD JNK2 isoforms (Fig. 1A). The neuronal JNK isoform (JNK3) was not detected (*5*). The compound mutant $Jnk1^{-/-}Jnk2^{-/-}$ MEF did not express JNK1 or JNK2. These data indicated that $Jnk1^{-/-}$ $Jnk2^{-/-}$ MEF may lack a functional JNK signal transduction pathway. This conclusion was confirmed by analysis of JNK activity in MEF exposed to ultraviolet (UV) radiation (Fig. 1B) or treated with fetal bovine serum (Fig. 1C). Disruption of the *Jnk1* and *Jnk2* genes did not alter expression of related mitogen-activated protein kinases (MAPK), ERK and p38, or the JNK activators MKK4 and MKK7 (Fig. 1A). The MKK4 and MKK7

[1]Howard Hughes Medical Institute, Program in Molecular Medicine, Department of Biochemistry & Molecular Biology, University of Massachusetts Medical School, Worcester, MA 01605, USA. [2]Howard Hughes Medical Institute, Section of Immunobiology, Yale University School of Medicine, New Haven, CT 06520, USA. [3]Department of Cell Biology, University of Massachusetts Medical School, Worcester, MA 01605, USA. [4]Department of Molecular Genetics and Microbiology, State University of New York at Stony Brook, Stony Brook, NY 11794, USA.

*Present address: Lilly Research Laboratories, Eli Lilly and Company, Indianapolis, IN 46285, USA.

†To whom correspondence should be addressed. E-mail: Roger.Davis@umassmed.edu

activity in *Jnk1*$^{-/-}$*Jnk2*$^{-/-}$ MEF after UV treatment was 66% and 77%, respectively, of that detected in WT MEF (*5*). UV-activated p38 MAPK (Fig. 1B) and serum-activated ERK (Fig. 1C) were detected in JNK-deficient cells. ERK activation was comparable in WT and *Jnk1*$^{-/-}$*Jnk2*$^{-/-}$ MEF, but a slight reduction of p38 MAPK activation was detected in *Jnk1*$^{-/-}$*Jnk2*$^{-/-}$ MEF. These data establish that *Jnk1*$^{-/-}$*Jnk2*$^{-/-}$ MEF possess no JNK and represent a useful model for studies of the JNK signaling pathway.

Jnk2$^{-/-}$ MEF proliferated slightly more rapidly in culture than did WT MEF (Fig. 1D). However, the saturation density of WT and *Jnk2*$^{-/-}$ MEF was similar. In contrast, *Jnk1*$^{-/-}$ MEF and compound mutant *Jnk1*$^{-/-}$ *Jnk2*$^{-/-}$ MEF proliferated more slowly than did WT cells and they reached a lower saturation density (Fig. 1D). The lower saturation density of these mutant MEF was observed at both low and high serum concentrations (Fig. 1E). These data indicated that JNK was required for normal proliferation of MEF and that JNK1 may be more important than JNK2 for proliferation. A greater role for JNK1 is consistent with the observation that *Jnk1* gene disruption caused a larger decrease in JNK activity than that caused by disruption of the *Jnk2* gene (Fig. 1, B and C). The reduced proliferation potential of MEF without JNK is similar to MEF without c-Jun (*6*) and MEF with a mutation in c-Jun that eliminated the JNK phosphorylation sites (*7*). This phenotypic similarity indicates that defects in c-Jun phosphorylation may contribute to the reduced proliferative potential of *Jnk1*$^{-/-}$ *Jnk2*$^{-/-}$ MEF.

The JNK signaling pathway has been implicated in the apoptotic response of cells exposed to stress (*8*). JNK is required for stress-induced neuronal apoptosis (*3, 7, 9*). However, the role of JNK in apoptosis of other cell types is controversial and the conclusions of several studies indicate that JNK may not mediate apoptotic signaling (*10*). Therefore we examined apoptosis of JNK-deficient MEF. WT and *Jnk2*$^{-/-}$ MEF exposed to UV exhibited decreased viability (Fig. 2A) and increased fragmentation of genomic DNA (Fig. 2B). Partial protection from UV-induced apoptosis was observed for *Jnk1*$^{-/-}$ MEF. *Jnk1*$^{-/-}$*Jnk2*$^{-/-}$ MEF were nearly completely protected from the effects of UV on survival (Fig. 2A), DNA fragmentation (Fig. 2B), and sub-G_1 DNA content (Fig. 2C). These data indicate that JNK is required for the normal apoptotic response of fibroblasts to UV. The partial protection observed for *Jnk1*$^{-/-}$ MEF was consistent with the lower amount of JNK activity detected in these cells after exposure to UV (Fig. 1B). The protection against UV-induced apoptosis caused by JNK deficiency was observed a long time after UV exposure (Fig. 2, A and B) and also in response to high doses of UV radiation (Fig. 2D). To confirm that the protection was caused by JNK deficiency, we examined the effect of *Jnk* gene dosage on UV-induced apoptosis. The amount of UV-induced apoptosis of *Jnk1*$^{-/-}$ MEF correlated with the amount of JNK expression (Fig. 2E). Treatment of MEF with a general caspase inhibitor (zVAD) prevented cell death caused by UV (Fig. 2F). In contrast, inhibitors of protein synthesis (cycloheximide) and mRNA synthesis (actinomycin D) did not inhibit UV-induced apoptosis. These data indicated that caspase activation, but not new gene expression, was required for UV-induced apoptosis. The absence of a requirement for new gene expression

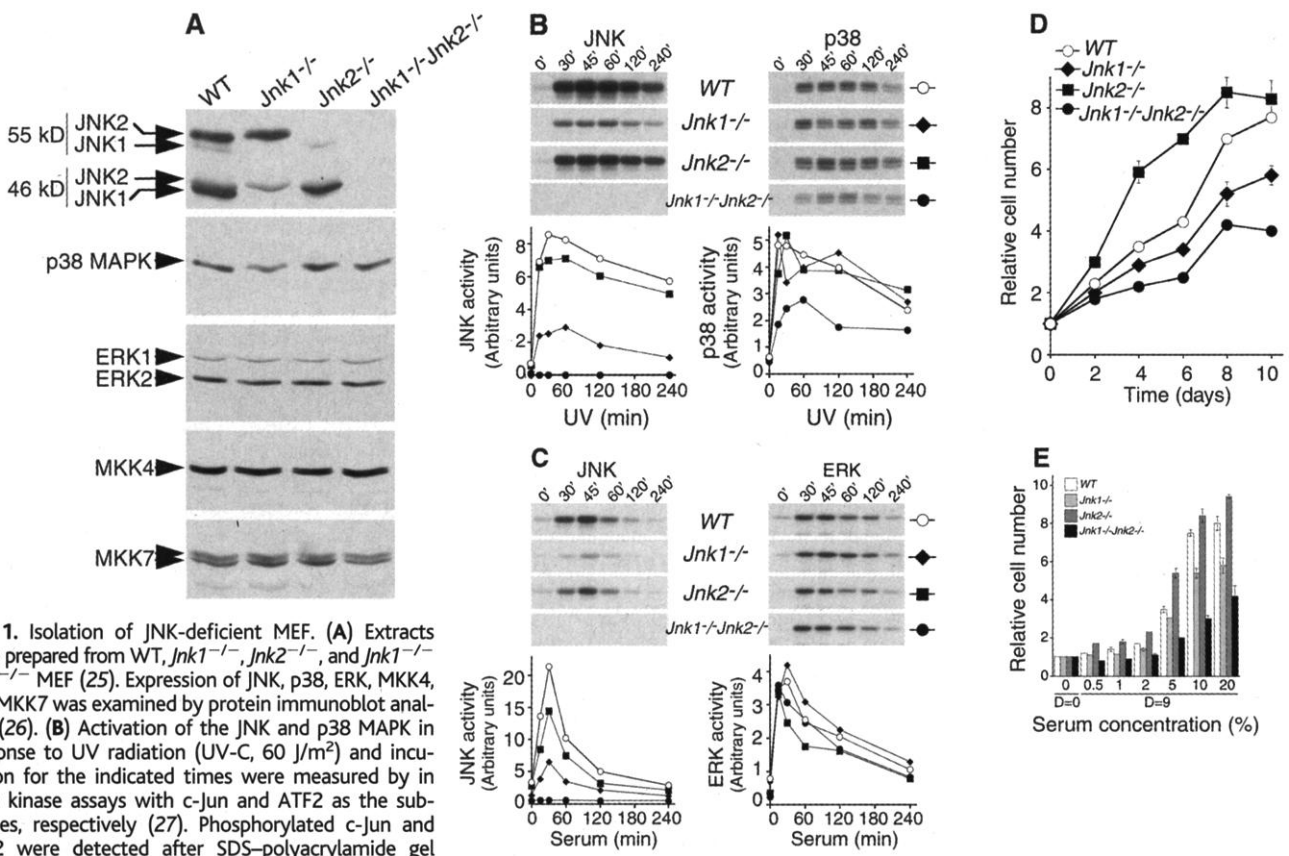

Fig. 1. Isolation of JNK-deficient MEF. (**A**) Extracts were prepared from WT, *Jnk1*$^{-/-}$, *Jnk2*$^{-/-}$, and *Jnk1*$^{-/-}$ *Jnk2*$^{-/-}$ MEF (*25*). Expression of JNK, p38, ERK, MKK4, and MKK7 was examined by protein immunoblot analysis (*26*). (**B**) Activation of the JNK and p38 MAPK in response to UV radiation (UV-C, 60 J/m^2) and incubation for the indicated times were measured by in vitro kinase assays with c-Jun and ATF2 as the substrates, respectively (*27*). Phosphorylated c-Jun and ATF2 were detected after SDS–polyacrylamide gel electrophoresis (PAGE) by autoradiography (upper), quantitated by PhosphorImager analysis (Molecular Dynamics), and are presented in arbitrary units (lower). (**C**) Activation of the JNK and ERK MAPK in response to treatment with fetal bovine serum (10%) and incubation for the indicated times were measured by in vitro kinase assays with c-Jun and c-Myc as the substrates, respectively (*27*). Phosphorylated c-Jun and c-Myc were detected after SDS-PAGE by autoradiography (upper), quantitated by PhosphorImager analysis (Molecular Dynamics), and presented as above (lower). (**D**) Proliferation of MEF was examined by crystal violet staining [mean optical density (OD) at 590 nm (±SD); $n = 3$] after addition of 1×10^4 cells to 20-mm tissue culture dishes and culture in medium supplemented with 10% fetal calf serum. (**E**) Saturation growth density of MEF in different concentrations of serum was examined by crystal violet staining [mean OD at 590 nm (±SD); $n = 3$]. Relative cell numbers were measured at day 0 ($D = 0$) and after culture for 9 days ($D = 9$).

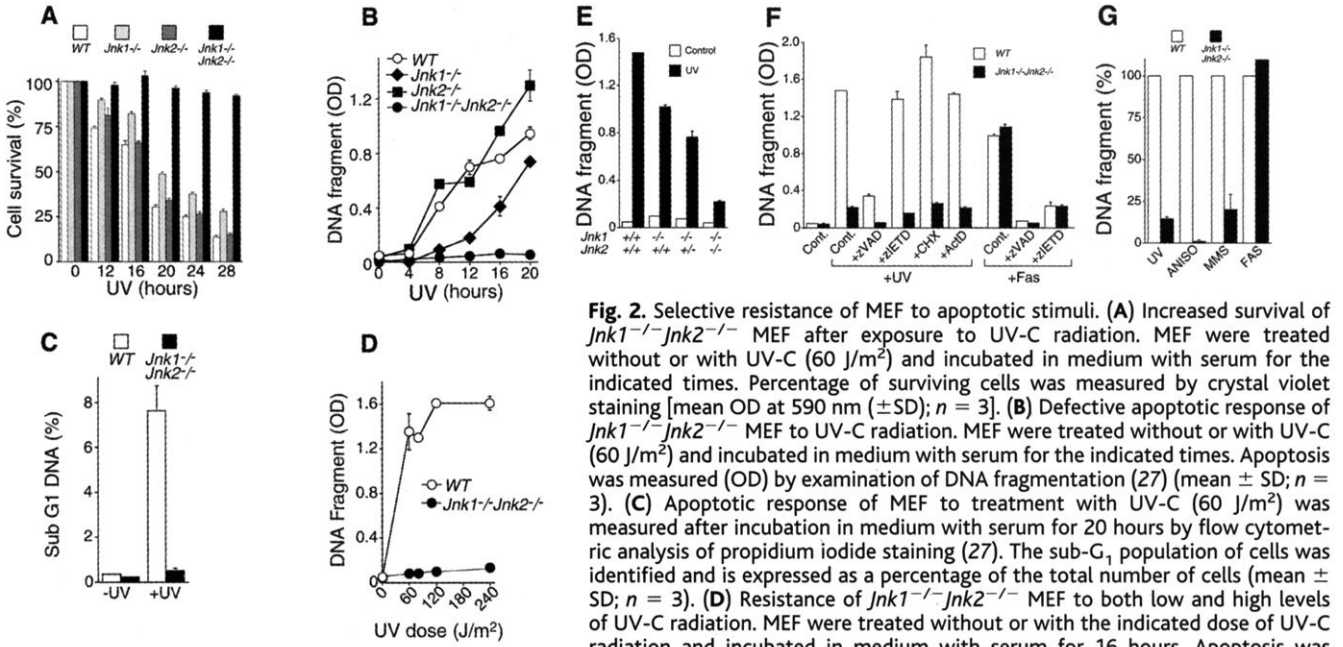

Fig. 2. Selective resistance of MEF to apoptotic stimuli. **(A)** Increased survival of *Jnk1*$^{-/-}$*Jnk2*$^{-/-}$ MEF after exposure to UV-C radiation. MEF were treated without or with UV-C (60 J/m^2) and incubated in medium with serum for the indicated times. Percentage of surviving cells was measured by crystal violet staining [mean OD at 590 nm (±SD); $n = 3$]. **(B)** Defective apoptotic response of *Jnk1*$^{-/-}$*Jnk2*$^{-/-}$ MEF to UV-C radiation. MEF were treated without or with UV-C (60 J/m^2) and incubated in medium with serum for the indicated times. Apoptosis was measured (OD) by examination of DNA fragmentation (*27*) (mean ± SD; $n = 3$). **(C)** Apoptotic response of MEF to treatment with UV-C (60 J/m^2) was measured after incubation in medium with serum for 20 hours by flow cytometric analysis of propidium iodide staining (*27*). The sub-G_1 population of cells was identified and is expressed as a percentage of the total number of cells (mean ± SD; $n = 3$). **(D)** Resistance of *Jnk1*$^{-/-}$*Jnk2*$^{-/-}$ MEF to both low and high levels of UV-C radiation. MEF were treated without or with the indicated dose of UV-C radiation and incubated in medium with serum for 16 hours. Apoptosis was measured (OD) by examination of DNA fragmentation (mean ± SD; $n = 3$). **(E)** Apoptotic defect of *Jnk1*$^{-/-}$*Jnk2*$^{-/-}$ cells is reduced by JNK expression. The effect of increasing amounts of JNK2 expression on apoptosis caused by UV-C (60 J/m^2) was examined after incubation in medium with serum for 16 hours by measurement of DNA fragmentation (mean ± SD; $n = 3$). **(F)** Requirement of caspases, but not new gene expression, for UV-C-induced apoptosis. MEF were untreated (Control) or were treated with UV-C (60 J/m^2; UV) or with anti-Fas (Jo2 antibody at 1 μg/ml plus cycloheximide at 0.3 μg/ml; Fas). The effect of pretreatment (2 hours) with zVAD (40 μM), zIETD (40 μM), cycloheximide (CHX; 0.3 μg/ml), or actinomycin D (ActD; 0.1 μg/ml) was examined. Cells were incubated in medium with serum for 16 hours and the amount of apoptosis was measured by analysis of DNA fragmentation (mean OD; $n = 3$). **(G)** *Jnk1*$^{-/-}$*Jnk2*$^{-/-}$ MEF are selectively resistant to proapoptotic stimuli. MEF were treated (16 hours) without and with UV-C (60 J/m^2; UV), anisomycin (5 μg/ml; ANISO), MMS (0.5 μM; MMS), or anti-Fas (Jo2 antibody at 1 μg/ml plus cycloheximide at 0.3 μg/ml; FAS). Apoptosis was measured (mean OD; $n = 3$) by examining DNA fragmentation. Amount of apoptosis measured for WT MEF exposed to each stimulus was normalized to a relative OD value of 100 (mean ± SD; $n = 3$).

distinguishes the JNK-dependent UV-induced apoptosis of MEF (Fig. 2F) from JNK-dependent excitotoxic stress-induced apoptosis of neurons, which requires c-Jun phosphorylation and new gene expression (*3, 7, 9*). We conclude that the JNK signaling pathway is required for the apoptotic response of fibroblasts to UV radiation.

The *Jnk1*$^{-/-}$*Jnk2*$^{-/-}$ MEF were also defective in the apoptotic response to the genotoxin methyl methanesulfonate (MMS) (Fig. 2G). Treatment with MMS caused apoptosis of WT cells. In contrast, *Jnk1*$^{-/-}$*Jnk2*$^{-/-}$ cells continued to proliferate after a period of growth arrest when exposed to MMS (*5*). The *Jnk1*$^{-/-}$*Jnk2*$^{-/-}$ MEF were also resistant to apoptosis caused by the drug anisomycin. In contrast, normal apoptosis of both WT and *Jnk1*$^{-/-}$*Jnk2*$^{-/-}$ MEF was observed in response to activation of the Fas death signaling pathway (Fig. 2G). These data indicate that JNK deficiency caused a selective defect in the apoptotic response of MEF.

The apoptotic defect in response to UV may be the consequence of increased survival signaling in *Jnk1*$^{-/-}$*Jnk2*$^{-/-}$ MEF. Therefore we examined activation of the transcription factor NF-κB and the protein kinase Akt (PKB), two important components of signaling pathways that promote cell survival (*11*). UV caused a similar increase in NF-κB DNA binding activity in WT and *Jnk1*$^{-/-}$*Jnk2*$^{-/-}$ MEF (*5*). In contrast, UV did not increase Akt activation [monitored with an antibody that recognizes phosphoserine-473 in Akt (*12*)] in WT or *Jnk1*$^{-/-}$*Jnk2*$^{-/-}$ MEF (*5*). These data indicate that increased survival signaling may not account for the resistance of *Jnk1*$^{-/-}$ *Jnk2*$^{-/-}$ MEF to UV-induced apoptosis.

The p53 tumor suppressor is negatively regulated by c-Jun (*6*) and JNK (*13*). Changes in p53 could contribute to the UV resistance and reduced proliferation of *Jnk1*$^{-/-}$ *Jnk2*$^{-/-}$ MEF because p53 is implicated in the cellular response to genotoxic stress (*14*). Therefore we examined the effect of UV on p53 in WT and *Jnk1*$^{-/-}$*Jnk2*$^{-/-}$ MEF. Exposure of WT and *Jnk1*$^{-/-}$*Jnk2*$^{-/-}$ MEF to UV caused reduced entry into S phase (Fig. 3A). Because radiation-induced growth arrest involves p53 (*14*), this observation indicates that p53 may function in *Jnk1*$^{-/-}$*Jnk2*$^{-/-}$ MEF. UV increased the amount of p53 (but not p73) in WT and *Jnk1*$^{-/-}$*Jnk2*$^{-/-}$ MEF (Fig. 3B). Immunofluorescence analysis demonstrated nuclear accumulation of p53 in WT and *Jnk1*$^{-/-}$*Jnk2*$^{-/-}$ MEF exposed to UV (*5*). The *Jnk1*$^{-/-}$*Jnk2*$^{-/-}$ MEF expressed slightly more p53 than did WT MEF and correlated with increased expression of p19^{ARF} and the cell cycle inhibitor p21 (Fig. 3B). Because p19^{ARF} stabilizes p53 by inactivating Mdm2 (*15*), the increased expression of p19^{ARF} may explain the increased amount of p53 and p53 target gene expression (p21) detected in *Jnk1*$^{-/-}$*Jnk2*$^{-/-}$ MEF. However, increased expression of Bax, another p53 target gene, was not observed (Fig. 3B). Thus, the reduced proliferation potential of *Jnk1*$^{-/-}$ *Jnk2*$^{-/-}$ MEF may be related, in part, to changes in p19^{ARF}, p53, and p21.

The caspase group of proteases is required for apoptosis (*16*). Therefore we examined whether JNK was required for caspase activation in response to UV. Gene knockout studies demonstrate that the initiator caspase required for Fas-induced death (caspase 8) is not required for UV-induced apoptosis (*17*). Thus, the caspase 8 inhibitor zIETD prevented Fas-induced, but not UV-induced, apoptosis (Fig. 2F). UV-induced cell death requires Apaf-1, the initiator caspase 9, and the effector caspase 3 (*18–20*). This pathway is initiated by the release of cytochrome c from the mitochondria (*21*). Therefore we examined the cytochrome c/Apaf-1/caspase 9/caspase 3 pathway in WT and JNK-deficient MEF. Caspase 3 activity was increased after exposure of WT MEF, but not *Jnk1*$^{-/-}$*Jnk2*$^{-/-}$ MEF, to UV (Fig. 4A). Protein immunoblot analysis confirmed that caspase 3 was processed from the proenzyme (32 kD) to the active form (18 kD) when WT MEF, but not *Jnk1*$^{-/-}$*Jnk2*$^{-/-}$ MEF, were exposed to UV (Fig. 4B). We also examined the

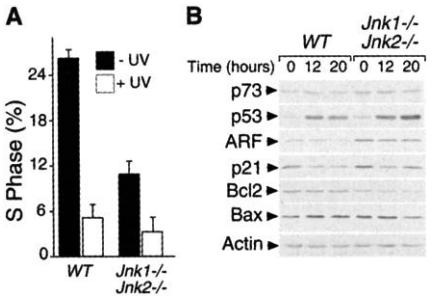

Fig. 3. Similar p53 response induced by UV radiation in WT and JNK-deficient MEF. (**A**) UV-C radiation causes growth arrest of WT and $Jnk1^{-/-}Jnk2^{-/-}$ MEF. MEF were treated without and with UV-C radiation (60 J/m^2) and incubated in medium with serum for 19 hours. Cells were pulse-labeled (1 hour) with BrdU, harvested, and examined by flow cytometry (*27*). The S-phase population of cells (labeled with BrdU) is presented as the percentage of total cells (mean ± SD; n = 3). (**B**) WT and $Jnk1^{-/-}Jnk2^{-/-}$ MEF were either untreated (0 hours) or exposed to UV radiation (60 J/m^2) and incubated in culture medium for 12 or 20 hours. Expression of p73, p53, ARF, p21, Bcl2, Bax, and actin was examined by protein immunoblot analysis (*26*).

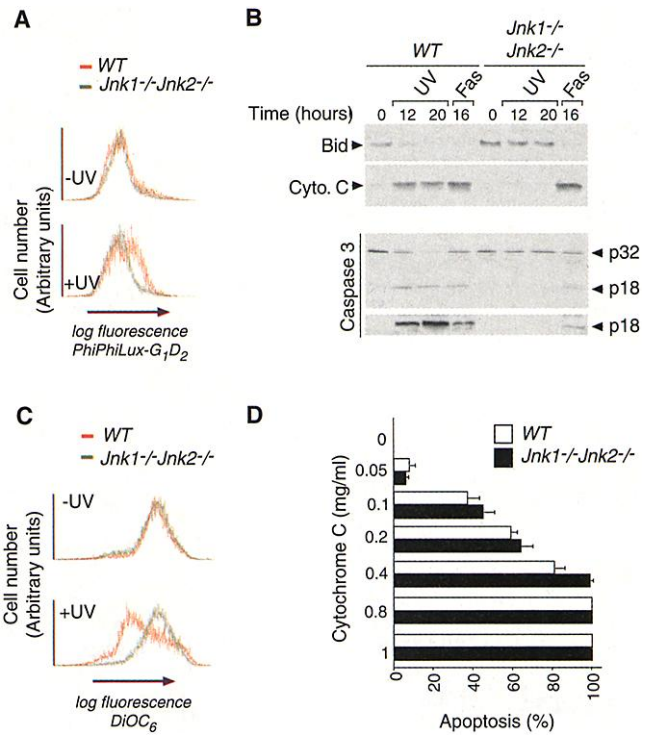

Fig. 4. Requirement of JNK for UV-C radiation-stimulated cytochrome c release and caspase activation. (**A**) Caspase 3 activity is increased after exposure of WT MEF, but not $Jnk1^{-/-}$ $Jnk2^{-/-}$ MEF, to UV-C radiation. WT (red) and $Jnk1^{-/-}Jnk2^{-/-}$ (green) MEF were exposed to UV radiation (60 J/m^2) and incubated in medium with serum for 15 hours. Caspase 3 activity was measured by incubating cells (1 hour) with the fluorogenic substrate PhiPhiLux-G_1D_2 and analyzing by flow cytometry (*27*). (**B**) Mitochondrial death pathway is activated by UV-C radiation in WT MEF but not in $Jnk1^{-/-}$ $Jnk2^{-/-}$ MEF. Cells were exposed to UV-C radiation (60 J/m^2) and incubated in medium with serum for 0, 12, and 20 hours. Effect of UV-C was compared with treatment (16 hours) with anti-Fas (Jo2 antibody at 1 μg/ml plus cycloheximide at 0.3 μg/ml; Fas). Expression of cytoplasmic cytochrome c (Cyto.C) and Bid was examined by protein immunoblot analysis. Caspase 3 was detected by protein immunoblot analysis of total cell extracts with a caspase 3 antibody that binds both procaspase 3 (p32) and activated caspase 3 (p18) (upper) and an antibody that specifically binds activated caspase 3 (p18) (lower). (**C**) UV-C radiation causes mitochondrial depolarization in WT MEF but not in $Jnk1^{-/-}Jnk2^{-/-}$ MEF. WT (red) and $Jnk1^{-/-}Jnk2^{-/-}$ (green) MEF were exposed to UV-C radiation (60 J/m^2) and incubated in medium with serum for 20 hours. Mitochondrial membrane potential was examined with the potentiometric dye 3,3′-dihexyloxacarbocyanine iodide [$DiOC_6(3)$] and analysis by flow cytometry (*27*). (**D**) Cytochrome c induces apoptosis in both WT MEF and $Jnk1^{-/-}Jnk2^{-/-}$ MEF. Cells were microinjected with fluorescein-conjugated dextran (3 mg/ml) and the indicated concentrations of cytochrome c (*28*). Apoptosis was scored 2 hours after injection. Averages of at least 150 cells from three independent determinations are shown. Error bars represent SD. Control experiments demonstrated that treatment of cells with the caspase inhibitor zVAD (40 μM) for 2 hours before microinjection reduced the cytochrome c–induced apoptosis.

release of mitochondrial cytochrome c. Exposure of WT MEF to UV caused a large increase in cytoplasmic cytochrome c (Fig. 4B) and decreased mitochondrial membrane potential (Fig. 4C). In contrast, UV did not cause cytochrome c release or mitochondrial depolarization in $Jnk1^{-/-}Jnk2^{-/-}$ MEF (Fig. 4, B and C). These defects in $Jnk1^{-/-}Jnk2^{-/-}$ MEF were selective for exposure to UV because Fas-induced cytochrome c release and caspase 3 processing were normal in JNK-deficient cells (Fig. 4B). Microinjection studies demonstrated that cytoplasmic cytochrome c caused apoptosis of both WT and JNK-deficient MEF (Fig. 4D). Selective resistance of $Jnk1^{-/-}Jnk2^{-/-}$ MEF to UV therefore reflects the failure of cytochrome c release from the mitochondria and caspase activation.

There are many possible targets of the JNK signaling pathway that may affect the mitochondria, including members of the Bcl2 group of apoptotic regulatory proteins (*22*). Indeed, the antiapoptotic protein Bcl2 has been reported to be phosphorylated and inactivated by JNK (*23*). However, an electrophoretic mobility shift, characteristic of phosphorylated Bcl2, was not detected in WT MEF exposed to UV radiation (Fig. 3B), which suggests that Bcl2 phosphorylation may not mediate the proapoptotic effects of UV-activated JNK. A second potential target of JNK signaling is Bid, a proapoptotic BH3-only member of the Bcl2 group, which is proteolytically activated to generate a fragment that translocates to the mitochondria and induces cytochrome c release (*24*). Fas caused Bid cleavage in both WT and $Jnk1^{-/-}$ $Jnk2^{-/-}$ MEF, but UV caused Bid cleavage only in WT MEF (Fig. 4B). The caspase inhibitor zVAD inhibited Bid cleavage and cytochrome c release caused by Fas, but not UV, indicating that Bid cleavage and cytochrome c release in response to UV may be caspase-independent (*5*). These data indicate that a BH3-only molecule (like Bid) is a possible mediator of proapoptotic signaling by JNK.

In conclusion, our study indicates that UV-induced apoptosis in fibroblasts requires JNK for cytochrome c release from the mitochondria. Other proteins required for UV-induced apoptosis include the cytochrome c effectors Apaf-1, caspase 9, and caspase 3 (*18*–*20*). Together with JNK, these proteins function as a signaling pathway that mediates UV-induced death.

References and Notes

1. D. L. Vaux and S. J. Korsmeyer, *Cell* **96**, 245 (1999).
2. G. Evan and T. Littlewood, *Science* **281**, 1317 (1998); J. Yuan and B. A. Yankner, *Nature Cell Biol.* **1**, E44 (1999).
3. D. D. Yang *et al.*, *Nature* **389**, 865 (1997).
4. D. D. Yang *et al.*, *Immunity* **9**, 575 (1998); C. Dong *et al.*, *Science* **282**, 2092 (1998); C. Y. Kuan *et al.*, *Neuron* **22**, 667 (1999).
5. C. Tournier, unpublished observation.
6. R. S. Johnson *et al.*, *Genes Dev.* **7**, 1309 (1993); M. Schreiber *et al.*, *Genes Dev.* **13**, 607 (1999).
7. A. Behrens, M. Sibilia, E. F. Wagner, *Nature Genet.* **21**, 326 (1999).
8. Y. T. Ip and R. J. Davis, *Curr. Opin. Cell Biol.* **10**, 205 (1998).
9. M. Dickens *et al.*, *Science* **277**, 693 (1997); Z. Xia *et al.*, *Science* **270**, 1326 (1995).
10. G. Natoli *et al.*, *Science* **275**, 200 (1997); Z. G. Liu *et al.*, *Cell* **87**, 565 (1996); A. Roulston *et al.*, *J. Biol. Chem.* **273**, 10232 (1998).
11. A. Khwaja, *Nature* **401**, 33 (1999).
12. J. Downward, *Curr. Opin. Cell Biol.* **10**, 262 (1998).
13. S. Y. Fuchs *et al.*, *Genes Dev.* **12**, 2658 (1998).
14. A. J. Giaccia and M. B. Kastan, *Genes Dev.* **12**, 2973 (1998).
15. J. D. Weber *et al.*, *Nature Cell Biol.* **1**, 20 (1999).
16. B. B. Wolf and D. R. Green, *J. Biol. Chem.* **274**, 20049 (1999).
17. P. Juo *et al.*, *Curr. Biol.* **8**, 1001 (1998); E. E. Varfolomeev *et al.*, *Immunity* **9**, 267 (1998).
18. M. Woo *et al.*, *Genes Dev.* **12**, 806 (1998); K. Kuida *et al.*, *Nature* **384**, 368 (1996).
19. R. Hakem *et al.*, *Cell* **94**, 339 (1998); K. Kuida *et al.*, *Cell* **94**, 325 (1998).
20. F. Cecconi *et al.*, *Cell* **94**, 727 (1998); H. Yoshida *et al.*, *Cell* **94**, 739 (1998).
21. H. Zou *et al.*, *Cell* **90**, 405 (1997); P. Li *et al.*, *Cell* **91**, 479 (1997).
22. A. Gross, J. M. McDonnell, S. J. Korsmeyer, *Genes Dev.* **13**, 1899 (1999).

23. K. Yamamoto, H. Ichijo, S. J. Korsmeyer, *Mol. Cell. Biol.* **19**, 8469 (1999); R. K. Srivastava *et al.*, *Proc. Natl. Acad. Sci. U.S.A.* **96**, 3775 (1999); K. Maundrell *et al.*, *J. Biol. Chem.* **272**, 25238 (1997); S. Haldar, N. Jena, C. M. Croce, *Proc. Natl. Acad. Sci. U.S.A.* **92**, 4507 (1995).
24. X. M. Yin *et al.*, *Nature* **400**, 886 (1999); H. Li, H. Zhu, C. J. Xu, J. Yuan, *Cell* **94**, 491 (1998); X. Luo *et al.*, *Cell* **94**, 481 (1998).
24. E. Bossy-Wetzel, D. D. Newmeyer, D. R. Green, *EMBO J.* **17**, 37 (1998).
25. MEF were prepared from day 13.5 embryos and cultured in Dulbecco's modified Eagle's medium supplemented with 10% fetal bovine serum (Life Technologies). All experiments were done with cells between passage 2 and passage 5. Similar data were obtained in experiments with independently isolated MEF.
26. Frozen cell pellets were lysed on ice (30 min) in RIPA buffer [50 mM tris-HCl (pH 7.5), 10 mM β-glycerophosphate, 5 mM EDTA, 150 mM NaCl, 1% Nonidet P-40, 1 mM phenylmethylsulfonyl fluoride, 1 mM sodium orthovanadate, aprotinin at 0.4 unit/ml, and leupeptin at 0.4 unit/ml]. Extracts (100 μg of protein) were examined by protein immunoblot analysis by probing with antibodies to PKB/AKT (New England Biolabs), p38 MAPK (Santa Cruz), ERK (Santa Cruz), JNK (Pharmingen), MKK4 (Santa Cruz), MKK7 (Zymed), p53 (Calbiochem), p73 (provided by W. G. Kaelin Jr.), ARF (Novus Biologicals), caspase 3 (Santa Cruz), active caspase 3 [A. Srinivasan *et al.*, *Cell Death Differ.* **5**, 1004 (1998)], p21 (Santa Cruz), Bcl2 (Pharmingen), Bax (Pharmingen), and actin (Calbiochem). S100 fractions were prepared [J. Yang *et al.*, *Science* **275**, 1129 (1997)] and examined by immunoblot analysis by probing with antibodies to cytochrome c (Pharmingen) and Bid (provided by X. Wang). Immune complexes were detected by enhanced chemiluminescence (Kirkegaard & Perry).
27. MAPK activity was measured by in vitro kinase assays [J. Raingeaud *et al.*, *J. Biol. Chem.* **270**, 7420 (1995)]. Apoptosis was examined by analysis of DNA fragmentation by the cell death detection ELISA method (Boehringer Mannheim). The percentage of cells in sub-G_1 and S phase was examined by flow cytometry analysis of bromodeoxyuridine (BrdU) incorporation and propidium iodide staining [F. Dolbeare *et al.*, *Methods Cell Biol.* **33**, 207 (1990)]. The mitochondrial membrane potential was examined by loading the cells (30 min at 37°C) with 40 nM 3,3'-dihexyloxacarbocyanine iodide (Molecular Probes) and analyzing by flow cytometry [R. M. Siegel *et al.*, *J. Cell Biol.* **141**, 1243 (1998)]. Caspase 3 activity was measured by incubating the cells for 1 hour with the fluorogenic substrate PhiPhiLux-G_1D_2 (Alexis Biochemicals) and analyzing by flow cytometry [D. M. Finucane *et al.*, *J. Biol. Chem.* **274**, 2225 (1999)].
28. Cells were plated onto gridded cover slips and maintained in Dulbecco's modified Eagle's medium containing 10% fetal calf serum for 2 days before injection. Fluorescein-conjugated dextran and cytochrome c (Sigma) were dissolved in phosphate-buffered saline and microinjected into the cytoplasm. Injected cells were identified by fluorescence microscopy and apoptosis was quantified by counting the number of injected cells immediately after injection and again 2 hours after injection. Apoptotic MEF aggregate and rapidly detach from the cover slip, which makes it impossible to score for individual apoptotic cells.
29. Supported in part by a grant from the National Cancer Institute. We thank our colleagues for providing reagents essential for this study, M. Woda for assistance with fluorescence-activated cell sorter analysis, and Kathy Gemme for expert administrative assistance. R.A.F. and R.J.D. are investigators of the Howard Hughes Medical Institute.

30 November 1999; accepted 25 February 2000

Ubiquitin Protein Ligase Activity of IAPs and Their Degradation in Proteasomes in Response to Apoptotic Stimuli

Yili Yang, Shengyun Fang, Jane P. Jensen, Allan M. Weissman, Jonathan D. Ashwell*

To determine why proteasome inhibitors prevent thymocyte death, we examined whether proteasomes degrade anti-apoptotic molecules in cells induced to undergo apoptosis. The c-IAP1 and XIAP inhibitors of apoptosis were selectively lost in glucocorticoid- or etoposide-treated thymocytes in a proteasome-dependent manner before death. IAPs catalyzed their own ubiquitination in vitro, an activity requiring the RING domain. Overexpressed wild-type c-IAP1, but not a RING domain mutant, was spontaneously ubiquitinated and degraded, and stably expressed XIAP lacking the RING domain was relatively resistant to apoptosis-induced degradation and, correspondingly, more effective at preventing apoptosis than wild-type XIAP. Autoubiquitination and degradation of IAPs may be a key event in the apoptotic program.

Thymocytes undergo apoptosis in response to many stimuli, including glucocorticoids, etoposide, γ-radiation, and engagement of their receptors for antigen (*1*). Reagents that inhibit proteasomes, multicatalytic protease complexes responsible for the degradation of ubiquitinated cellular proteins (*2*), block cell death induced by many of these stimuli (*3*). One possible explanation is that proteasome-mediated degradation of anti-apoptotic proteins might be required for cell death to occur. Candidate anti-apoptotic molecules expressed in immature thymocytes include the Bcl-2 family member Bcl-x_L and members of the IAP (inhibitors of apoptosis) family (*4*). To explore this idea, we induced thymocytes to die by treating them with dexamethasone (Dex). Under these conditions, amounts of both c-IAP1 (inhibitor of apoptosis–1) and XIAP (X-linked inhibitor of apoptosis) were substantially decreased (Fig. 1A) (*5*). No change occurred in amounts of Bcl-x_L or β-actin. An increase in Dex-induced cell death was not observed until 8 hours of culture, and even at this time ~90% of thymocytes were viable (Fig. 1B). Inhibition of proteasome activity greatly reduced apoptosis at 16 hours (Fig. 1B) (*3*). Amounts of c-IAP1 and XIAP began to decrease 4 to 6 hours after culture with Dex, and by 8 hours were decreased by 64 ± 1.7% for cIAP-1 (n = 3) and 73 ± 3.4% for XIAP (n = 5) (Fig. 1D) (*6*). Etoposide is a topoisomerase II inhibitor that, unlike glucocorticoids, induces apoptosis through a p53-dependent pathway (*7*). Etoposide induced a decrease in IAP levels that was first observed after 2 to 4 hours of culture, and by 6 hours the amounts of c-IAP1 and XIAP fell ~87 ± 7.5% (n = 3) and 77 ± 8.5% (n = 5), respectively (Fig. 1E) (*6*). Cell death was first detected by trypan blue exclusion ~8 hours after addition of etoposide and was largely prevented in cells treated with proteasome inhibitors (Fig. 1C). Therefore, induction of apoptosis by two different afferent pathways resulted in relatively early and specific loss of IAPs in thymocytes.

The relatively rapid decrease in the amount of IAPs in thymocytes stimulated to undergo apoptosis raised the possibility that these proteins were being targeted for degradation. Given that the proteasome is a major effector of intracellular protein degradation and that proteasome inhibitors block glucocorticoid- and etoposide-induced thymocyte apoptosis (*3*) (Fig. 1), thymocytes were cultured with Dex or etoposide in the absence or presence of proteasome inhibitors (Fig. 2). Both a peptide aldehyde proteasome inhibitor and the highly specific proteasome inhibitor lactacystin effectively blocked the decrease in IAP expression induced by the apoptotic stimuli.

Protein ubiquitination involves the sequential action of ubiquitin activating enzyme (E1), a ubiquitin-conjugating enzyme (E2), and a ubiquitin protein ligase (E3) (*8*). Ubiquitination by some known E3's and several proteins of previously unknown function is dependent on an intact RING finger (*9*, *10*). IAPs contain a COOH-terminal RING domain, so we examined whether these molecules also have ubiq-

Laboratory of Immune Cell Biology, Division of Basic Sciences, National Cancer Institute, National Institutes of Health, Bethesda, MD 20892, USA.

*To whom correspondence should be addressed. E-mail: jda@box-j.nih.gov